Thermal and Kinetic Behaviors of Fallen Leaves and Waste Tires Using Thermogravimetric Analysis

Shukai Shi, Xiaoyan Zhou,* Weimin Chen, Xin Wang, Thiphuong Nguyen, and Minzhi Chen

Thermal decomposition characteristics and kinetic parameters of fallen leaves (FLs), waste tires (WTs), and their blends (1:1 weight ratio) were investigated. Pyrolysis experiments were conducted with four different heating rates of 5 °C/min, 10 °C/min, 20 °C/min, and 40 °C/min from 35 °C to 800 °C in a nitrogen atmosphere using a thermogravimetric analysis (TGA). The thermogravimetry/derivative thermogravimetry (TG/DTG) curves indicated that the three samples were mainly degraded in a wide temperature range of 350 °C to 450 °C, and that a greater weight loss rate corresponded to a higher heating rate. An elemental analysis demonstrated that FLs/WTs blends embraced a maximum calorific value that reached 25.24 MJ/kg. Two model-free methods, iso-conversional Kissinger-Akahira-Sunose (KAS) and Flynn-Wall-Ozawa (FWO) were applied on the TGA data of samples to calculate the activation energies. The results showed that the average activation energies of the same feedstock based on KAS and FWO methods were approximately the same, with the highest error within 1.6%. Then, the activation energies obtained were introduced in the Coats/Redfern (CR) model-fitting method to derive the pre-exponential factors, based on first order rate of reaction.

Keywords: Fallen leaves; Waste tires; Pyrolysis; TGA; Kinetic

*Contact information: College of Materials Science and Engineering, Nanjing Forestry University, Nanjing 210037, China; *Corresponding author: zhouxiaoyan@njfu.edu.cn*

INTRODUCTION

There is a trend that humans' energy demands are increasing, whereas fossil fuel resources are decreasing. A survey of the literature available shows that the total fossil fuel reserves will be consumed gradually after 2042 (Shafiee and Topal 2009). Therefore, it is necessary to seek alternative resources that are clean, sustainable, and renewable. Biomass, like municipal waste fallen leaves, as a potential carbon-neutral source of energy, has tremendous value for exploitation and utilization (El-Sayed and Mostafa 2015). The utilization of biomass has become an advanced research hotspot in most rising developing economies due to a large amount of energy needs. Pyrolysis is widely accepted as a very promising and viable thermochemical conversion technology. It can quickly lead to some effective transformations, such as biomass-to-energy or biomass-to-higher-value products, in comparison with the conventional methods of disposal (Bridgewater and Anthony 2004). Also, biomass materials can be converted into various types of fuels, such as liquid, char, and gas that are suitable for marketing directly. Furthermore, the pyrolysis of biomass can contribute indirectly to avoiding the emission of chemical pollution caused by the use of fossil fuels, because biomass universally contains lower levels of nitrogen and sulfur and the thermal degradations of biomaterials are generally executed under a complete absence of oxygen gas environment (Chen *et al.* 2014c).

Nevertheless, one of the fundamental by-products of biomass pyrolysis, namely bio-oil, has more disadvantages than advantages with respect to its current application as bio-fuels (Oasmaa 1999). This restriction follows from the chemical and physical properties of bio-oil itself. Bridgwater reported that the bio-oil was composed of 45 wt.% to 50 wt.% oxygenated compounds and thus this substance exhibited chemical instability and corrosion (Bridgwater 2004, 2012). Also, the characteristics of high viscosity and poor ignition must be unfavorable for its industrialization (Oasmaa 1999). Thus, it is necessary to improve the quality of bio-oils by means of some upgrading techniques. Considering the cost and implementation complexity of catalytic hydro-dearomatization or chemical deoxygenation, an increasing number of researchers are trying to study and develop simple, cheap, and efficient co-pyrolysis of biomass with a polymer (Abnisa and Wan 2014; Chen *et al.* 2016b). Brebu *et al.* (2010) concluded that the co-pyrolysis of pine cones with synthetic polymers, including low-density polyethylene (LDPE), polypropylene (PP), and polystyrene (PS), could obtain higher yields of liquids than theoretical yields. Relative to the co-pyrolysis of biomass with plastics, approximately 1.5 billion tires are produced worldwide annually, and they are eventually treated as waste (Williams 2013). Waste tires, which are primarily composed of rubber and carbon black, have been applied to industrial pyrolysis for producing around 63 wt.% liquid yield with high caloric value that resulted from a high H/C atomic ratio containing a low oxygen content, and aromatic and aliphatic compounds (Martínez *et al.* 2013; Quek and Balasubramanian 2013). A recent study has shown that the addition of waste tires into biomass materials during pyrolysis can be conducive to the improvements in the oils quality and quantity as a result of a synergistic effect in existence *via* free radical interactions (Martínez *et al.* 2014; Uçar and Karagöz 2014). Consequently, the pyrolysis of bio-based materials blended with fossil-based waste tires is an optional technique to achieve high-grade fuels (Abnisa and Wan 2014; Chen *et al.* 2016a).

The objective of this study was to investigate the thermal behavior of fallen leaves, waste tires, and their blends, and evaluate the three samples' kinetic triplets, namely activation energy (E), pre-exponential factor (A), and reaction order (n) under non-isothermal conditions. These parameters may serve to optimize the design of the reactor by exploring reaction mechanisms that control the process of a pyrolysis reaction well when using these types of feedstocks (Çepelioğullar *et al.* 2015). The obtained data were calculated in the manner of a reliable and suitable kinetic model.

Table 1. Definitions of Symbols

A	Pre-exponential factor (s^{-1})	β	Heating rate (k/min^{-1})
E	Activation energy (kJ mol^{-1})	α	Pyrolysis conversion
R	Gas constant (8.314 J mol^{-1} k^{-1})	K	Reaction rate constant (min^{-1})
R^2	Correlation coefficient	t	Time (min)
n	Reaction order	m_0	Initial sample weight (mg)
$f(\alpha)$	Reaction mechanism function	m_t	Sample weight at a given time (mg)
T	Absolute temperature (k)	m_f	Final sample weight (mg)
T_α	Temperature at a particular conversion (k)	$(dw/dt)_{max}$	Maximum degradation rate (%/min)

EXPERIMENTAL

Materials

The representative biomass materials of fallen leaves (FLs) were adopted in the study of pyrolysis because of their local availability and the difference between lignocellulosic biomasses in terms of their heterogeneous nature. The FLs were collected from phoenix trees at Nanjing Forestry University (Nanjing, China). Before the test, these leaves were cleaned up and ground into a particle size of 60- to 80-mesh (0.25 mm to 0.18 mm), then the samples were dried at 103 °C for 6 h (Rivilli *et al.* 2011). The purified waste tires (WTs) with an average particle size of 1.5 mm were provided from a waste rubber recycling plant in Nanjing (China) (Uçar and Karagöz 2014). The ultimate analyses of FLs, WTs, and their blends were performed by an elemental analyzer (2400 II, Perkin Elmer Inc., Waltham, USA)

Methods

Experimental procedure

After pretreating raw materials, the FLs were mixed with WTs uniformly in a weight ratio of 1:1 using an agate mortar for further co-pyrolysis. In addition, two kinds of remaining ingredients would be operated separately under identical conditions for comparison.

Pyrolysis alone and co-pyrolysis experiments were performed in a thermogravimetric analyzer (STA209F3, Netzsch Group, Bavaria, Germany), that could characterize the mass loss of a sample with time and temperature during a continuous heating process. For each experiment, approximately 5 mg to 10 mg of sample was loaded into a ceramic crucible and then fed into an inert gas of high-purity nitrogen (99.99%) with a steady flow rate of 80 mL/min, which could be used to prevent sample combustion and to sweep off hot vapors. Subsequently, the temperature was programmed and set precisely for running at a range from 35 °C to 800 °C. After that, the FLs/WTs blends and the individual components of fallen leaves and waste tires were pyrolyzed at four different heating rates of 5 °C/min, 10 °C/min, 20 °C/min, and 40 °C/min as a function of newly released research findings (Zhu *et al.* 2015).

Kinetic theory

The main content of the present work employed a validated model to determine the kinetics parameters in a form of mathematical equations. Here Eq. 1 is the basic expression with respect to thermal decomposition kinetics (Gustafsson and Richards 2009),

$$\frac{d\alpha}{dt} = f(\alpha)k(t) \quad (1)$$

where $f(\alpha)$ represents the reaction mechanism function, defined as $f(\alpha) = (1-\alpha)^n$, which is related with the degree of pyrolysis conversion, namely α ($\alpha = (m_0 - m_t)/(m_0 - m_f)$). The mass is measured by thermogravimetric analyzer called m_0 (mg), m_t (mg), and m_f (mg) are the initial sample weight, sample weight at a given time, and the final sample weight, respectively. The variable K is the reaction rate constant expressing the dependence on temperature, usually given in Eq. (2) by the Arrhenius formula (White *et al.* 2011):

$$K = A\exp(-E/RT) \quad (2)$$

The A (min^{-1}) is the pre-exponential factor, E (kJ mol^{-1}) is the activation energy, T is the absolute temperature (k), and R is known as the gas constant (8.314 J mol^{-1} k^{-1}).

For the non-isothermal TG experiment with a linear heating rate, β (k min^{-1}) can be described as Eq. 3,

$$\beta = \frac{dT}{dt} = \frac{dT}{d\alpha} \times \frac{d\alpha}{dt} \quad (3)$$

Hence Eq. 1 can be rewritten in a normalized form representing the TGA curve as following,

$$\frac{d\alpha}{dT} = \frac{A}{\beta} f(\alpha) \exp(-E/RT) \quad (4)$$

Finally, with integration and recombination of Eq. 4, it can be deduced as an integral function $g(\alpha)$ (Çepelioğullar *et al.* 2015):

$$g(\alpha) = \int_0^{\alpha} \frac{d\alpha}{f(\alpha)} = \frac{A}{\beta} \int_{T_0}^{T} \exp(-E/RT)dT \quad (5)$$

In the relevant literature, by introducing u, which is equal to E/RT (Montiano *et al.* 2016), and if setting $g(\alpha) = \int_0^{\infty} \frac{d\alpha}{f(\alpha)}$, then Eq. 5 can be rearranged as,

$$g(\alpha) = \int_0^{\infty} \frac{d\alpha}{f(\alpha)} = \frac{AE}{\beta R} \int_u u^{-2} e^{-u} = \frac{AE}{\beta R} P(u) \quad (6)$$

In the above Eq. 6, $P(u)$ is only an approximate integral solution applied to derive different iso-conversional forms (Ceylan and Topçu 2014).

Model-free methods, the KAS model

The expression of the Kissinger-Akahira-Sunose (KAS) method is transformed from Eq. 6 *via* using an approximation of $P(u) \cong u^{-2}e^{-u}$ to replace, and the final equation is simplified as the following (Ceylan and Topçu 2014),

$$\ln\left(\frac{\beta}{T_{\alpha}^2}\right) = \ln\left(\frac{AE}{Rg(\alpha)}\right) - \frac{E}{RT_{\alpha}} \quad (7)$$

This iso-conversional method allows the multi-grouping of experiments at different heating rates (β), where $T\alpha$ represents the temperature at a particular conversion. According to the plot of $\ln(\beta/T_{\alpha}^2)$ *versus* $1/T_{\alpha}$, the value of activation energy can be obtained by calculating the slope of a correlative line that is $-E/R$.

The FWO model

The Flynn-Wall-Ozawa (FWO) method evolved from Doyle's approximation ($\log P(u) \cong -2.315 - 0.4567u$) and took the logarithm of ten as the base (Doyle 2003; Wang and Zhao 2016):

$$\log \beta = \log\left(\frac{AE}{Rg(\alpha)}\right) - 2.315 - 0.4567\frac{E}{RT_\alpha} \quad (8)$$

For Eq. 8, by plotting a linear graph of logβ *versus* $1/T_\alpha$, the slope of the straight line represents $-0.4567E/R$, which can be used to obtain the activation energy.

Model-fitting method

Using the Coats-Redfern model of Eq. 9 and assuming the reaction order is 1, the pre-exponential factor can be calculated as (Cao *et al.* 2016),

$$\ln\left(\frac{-\ln(1-\alpha)}{T^2}\right) = \ln\left(\frac{AR}{\beta E}\right) - \left(\frac{E}{RT}\right) \quad (9)$$

RESULTS AND DISCUSSION

Characterization of Raw Materials

The energy content of the fuels is highly correlated to their amounts and types of chemical contents (carbon, hydrogen, and oxygen, *etc.*) (El-Sayed and Mostafa 2014). Results of the ultimate analyses are listed in Table 2. The data indicated that FLs/WTs mixtures contained a higher carbon and hydrogen content compared to single FLs and WTs, whereas the oxygen content was less than the first two. After WTs were mixed with biomass fallen leaves, the sulfur content was reduced, which cut down the emission of toxic gases during pyrolysis (Martínez *et al.* 2014). Finally, with the help of the measured carbon, hydrogen, oxygen, and sulfur contents, the calorific values of FLs, WTs, and their blends were calculated as 16.61 MJ/kg, 23.81 MJ/kg, and 25.24 MJ/kg, respectively. The ultimate analysis provides a proof that the FLs/WTs combinations can benefit to increase the calorific value. Therefore, it is further established that FLs/WTs is a viable and potential candidate for a resource of energy and chemicals (Abnisa and Wan 2014).

Table 2. Ultimate Analysis of the FLs, WTs, and FLs/WTs (wt.%, dry basis)

Material and Property	FLs	WTs	FLs/WTs
Carbon	46.88	62.54	62.73
Hydrogen	6.08	5.41	6.25
Oxygen [a]	44.66	29.13	28.11
Nitrogen	1.98	1.8	2.13
Sulfur	0.4	1.12	0.78
Calorific Value (MJ/kg) [b]	16.61	23.81	25.24
[a] By difference (Chen *et al.* 2014b)			
[b] Calculated by using (338.2 x C) + (1442.8 x (H - (O / 8))) + (94.2 x S) (Çepelioğullar and Pütün 2013)			

Thermogravimetric Analysis

The thermogravimetry (TG) and derivative thermogravimetry (DTG) curves of FLs, WTs, and their blends are given in Fig. 1. Table 3 also lists the concrete data of the thermal

behavior of three samples for each of the heating rates. As shown in Fig. 1a, it was evidently found that the whole process of thermal decomposition of FLs could be divided into three stages.

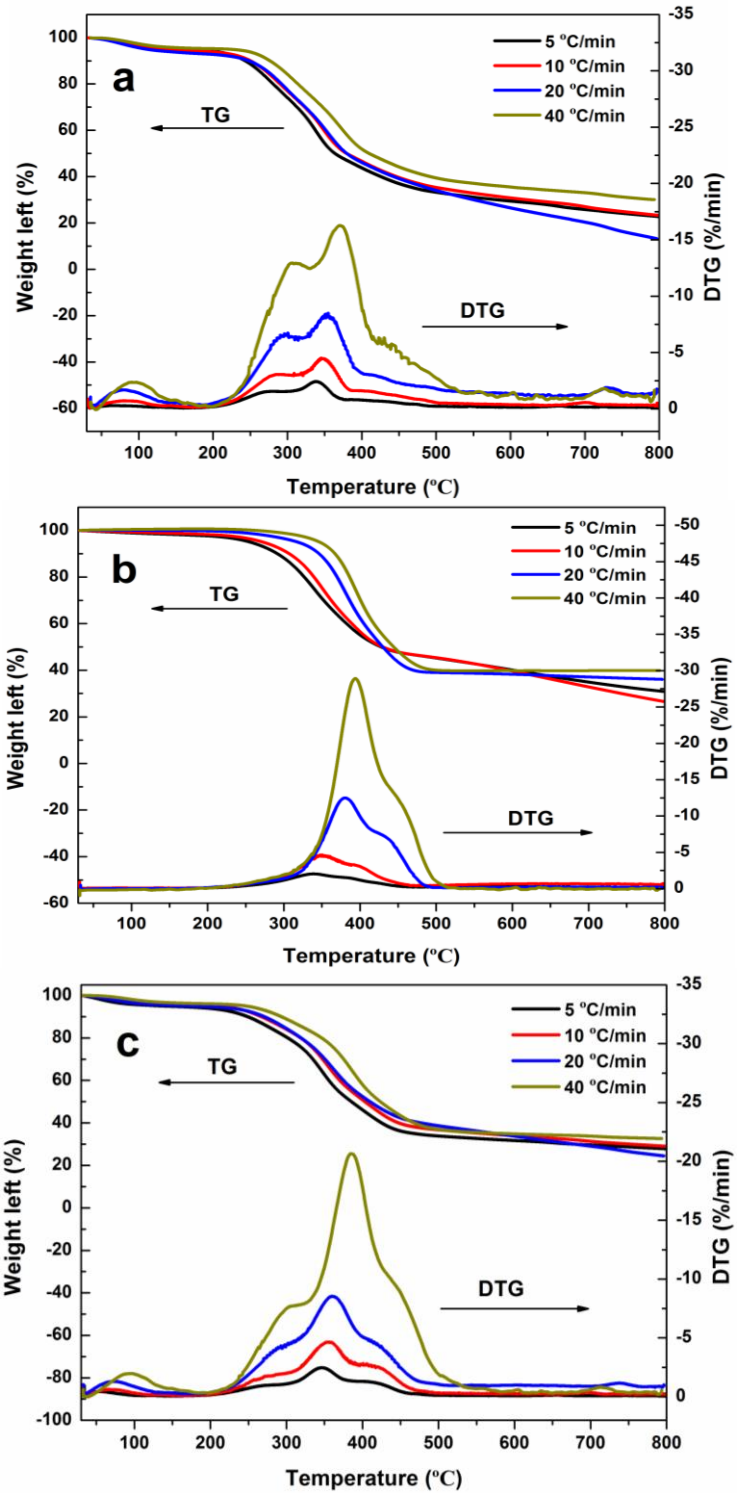

Fig. 1. The TG and DTG curves of each feedstock and their blends at heating rates of 5, 10, 20, and 40 °C/min; (a) FLs, (b) WTs, and (c) FLs/WTs

To begin with, the first stage signified the removal of internal moisture and a small amount of volatile matter from the raw material (Çepelioğullar *et al.* 2015; El-Sayed and Mostafa 2015). Thereafter, when the temperature approached 200 °C, the FLs underwent a second stage of thermal weight loss at all heating rates, where the hemicellulose and cellulose started to decompose. As the heating continued, the main weight loss stage could be clearly distinguished between 310 °C and 500 °C, where the decomposition temperature that corresponded to the maximum weight loss rate of the material tended to move towards a higher temperature with the increased heating rate. This phenomenon is called thermal lag (Chin *et al.* 2014). Because a higher heating rate decreased the residence time of the biomaterial at each temperature point, it resulted in a poor degree of reaction progress. Thus, the temperature at the maximum pyrolysis rate was backwards (Wang and Zhao 2016). At this stage, the hemicellulose and cellulose underwent complete degradation and the lignin was gradually transformed into coke (Abnisa and Wan 2015; Montiano *et al.* 2016). Meanwhile, the recorded maximum weight loss rates were 2.4, 4.4, 8.3, and 16.3 %/min, corresponding to the 5, 10, 20, and 40 °C/min in this region.

Figure 1b is a thermogram of WTs and illustrates that the decomposition took place in almost a single step. The degradation area started at 261 °C and ended at 510 °C, which was consistent with the fact that the natural rubber decomposed at a lower temperature, and the curve extended up to the range corresponding to decomposition of styrene-butadiene rubber at a higher temperature (Martínez *et al.* 2014; Uçar and Karagöz 2014). In particular, the weight loss rate of WTs under the condition of 40 °C/min was 28.9 %/min, which was 2.5, 6, and 14 times more corresponding to the heating rate of 20, 10, and 5 °C/min, respectively. It was noticeable that the degradation temperature of WTs varied with the increased heating rate, which was the same as the thermal behavior of the FLs.

Based on Fig. 1c, it might be inferred that the FLs interacted with the WTs during their co-pyrolysis (Zhou *et al.* 2009). For example, contrasting to the quantity of final residue produced by pyrolysis, it can be seen that the mixture matrix (FLs/WTs) was superior to single FLs for all heating rates. The might be explained by assuming that the pyrolysis of the blends generated some intermediates (Zhou *et al.* 2009). Accordingly, the weight loss reduced. Likewise, it was also observed that in the temperature range of 300 °C to 400 °C, the peak value of the DTG curves of the mixture was higher than the FLs under the same heating rate. When comparing the thermal decomposition behavior of WTs and the mixture, it was fairly easy to spot a difference in the onset temperature of the primary decomposition between the two materials. That is, the mixture started to decompose at approximately 213 °C, whereas the WTs began after 300 °C. This could have been attributed to the process of mixture decomposition that involved the pre-decomposition of cellulose and hemicellulose (Doyle 2003). Furthermore, to better understand the interactions taking place, an equation which could quantitatively describe the extent of the synergistic effect in different heating rates was defined as difference of weight loss $\Delta W = W_m - (X_1 * W_1 + X_2 * W_2)$, where W_m, W_1, and W_2 represent the weight loss of mixture, FLs and WTs separately, and X_1 and X_2 are the mass fraction of each material (Uzun and Yaman 2014). In Fig. 2, it is observed that in the temperature range of about 330 °C to 480 °C, the ΔW reached a relative peak at heating rates of 20, 10, and 5 °C/min, which implied strong interactions between two pure materials (Chin *et al.* 2014). However, with the heating rate of 40 °C/min, the ΔW for the mixture was between -2% and -4% over the whole temperature scope, which indicated poor interactions between the FLs and WTs, despite ΔW not being equal to zero under this operating condition (Cai *et al*. 2008).

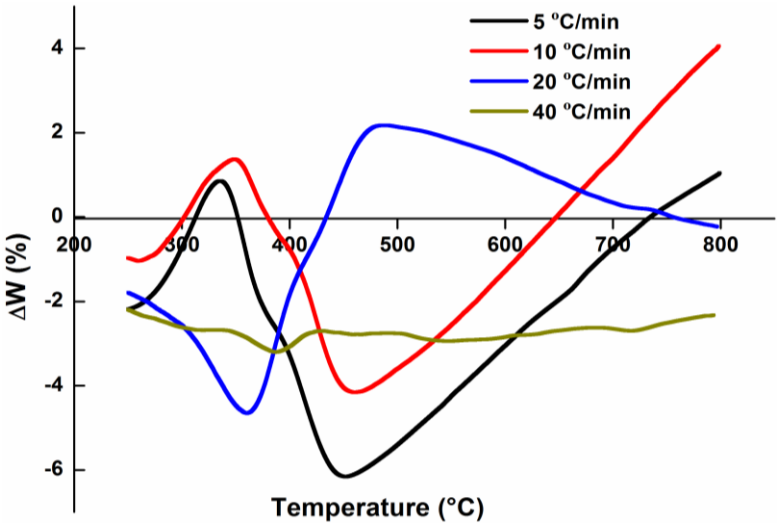

Fig. 2. Variation of Δw for FLs/WTs mixtures at different heating rates

Table 3. Pyrolysis Characteristics of Each Sample at Different Heating Rates

Sample	Heating Rate (°C/min)	Peak Temperature (°C)			$(dw/dt)_{max}$ (%/min)	Residue (%)
		First Stage	Second Stage	Third Stage		
FLs	5	103	269	338	2.4	22.7
	10	95	284	346	4.4	23.3
	20	78	298	353	8.3	13.6
	40	86	305	371	16.3	30.0
WTs	5	335	-	-	2.0	30.9
	10	349	-	-	4.5	26.6
	20	381	-	-	12.5	36.1
	40	393	-	-	28.9	39.9
FLs/WTs	5	64	265	346	2.5	27.8
	10	69	275	355	4.6	28.9
	20	65	288	360	8.5	24.4
	40	92	305	385	20.6	32.6

Kinetic Analysis

To acquire reliable kinetic parameters of the three samples, two different (KAS and FWO) models were utilized to determine the activation energy based on a specific scope of the pyrolysis conversion (Ma *et al.* 2015), as well as the CR model to calculate the pre-exponential factors (Huang *et al.* 2015).

First, the activation energy value was obtained separately by the help of the KAS model and the FWO model mentioned in Eqs. 7 and 8, taking the α value in the range of 0.1 to 0.5 into account. Figures 3 and 4 show the kinetic plots of different samples for each degree of conversion with a good agreement to the experimental data. From the slope (-*E*/*R*) of each straight line, the activation energy of the process and their corresponding correlation coefficients (R^2) were calculated in Table 4.

It can be seen that the maximum error of average activation energy of two model-free methods was less than 1.6%, in spite of the calculation of FWO being slightly higher than that of KAS. Also, it can be observed that the activation energy value of independent waste tires pyrolysis was the largest. This could be explained by the disproportionation or cyclisation reaction of polymer chains (Zhou *et al.* 2009; Mui *et al.* 2010).

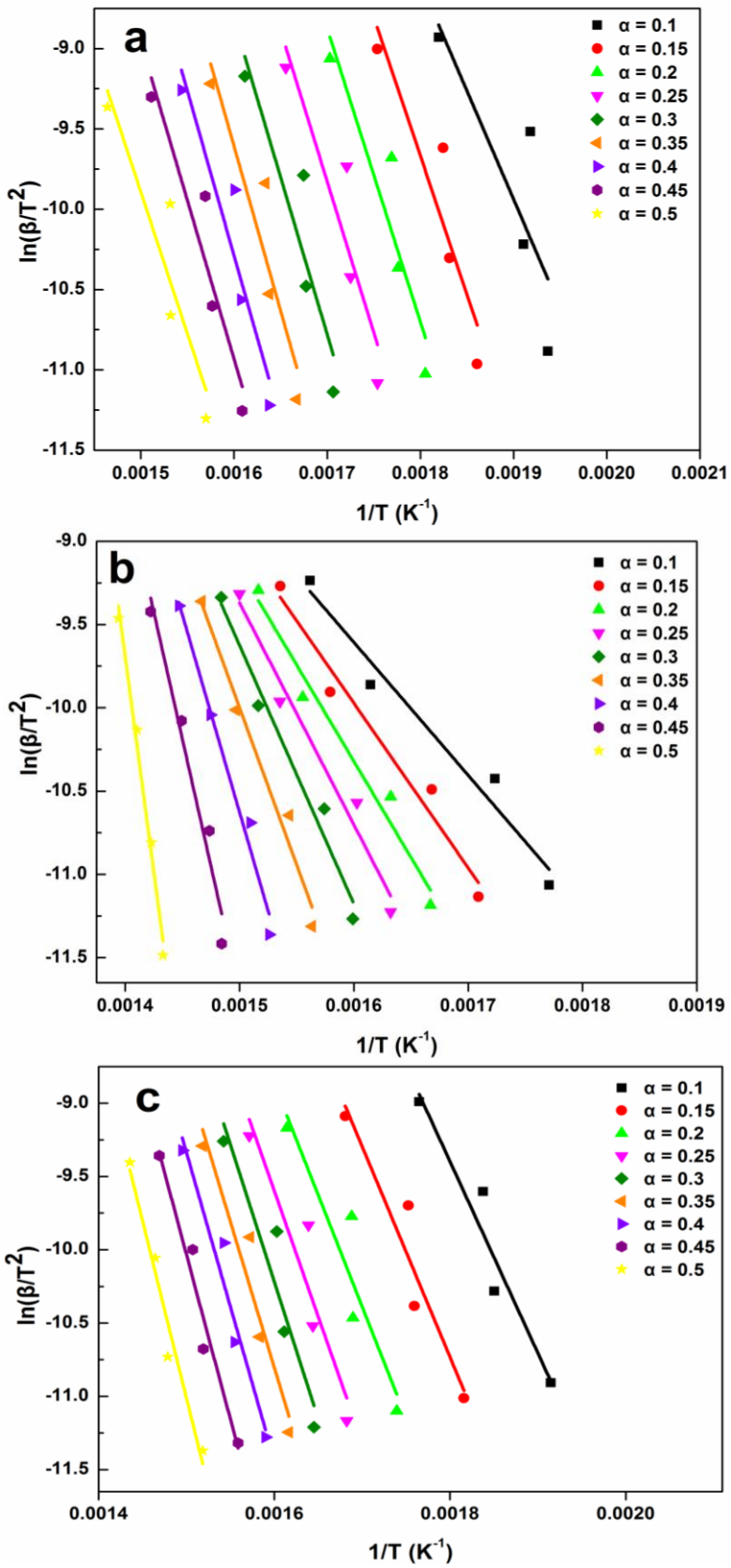

Fig. 3. Kinetic plots for determination of activated energy using KAS model at different conversions; (a) FLs, (b) WTs, and (c) FLs/WTs

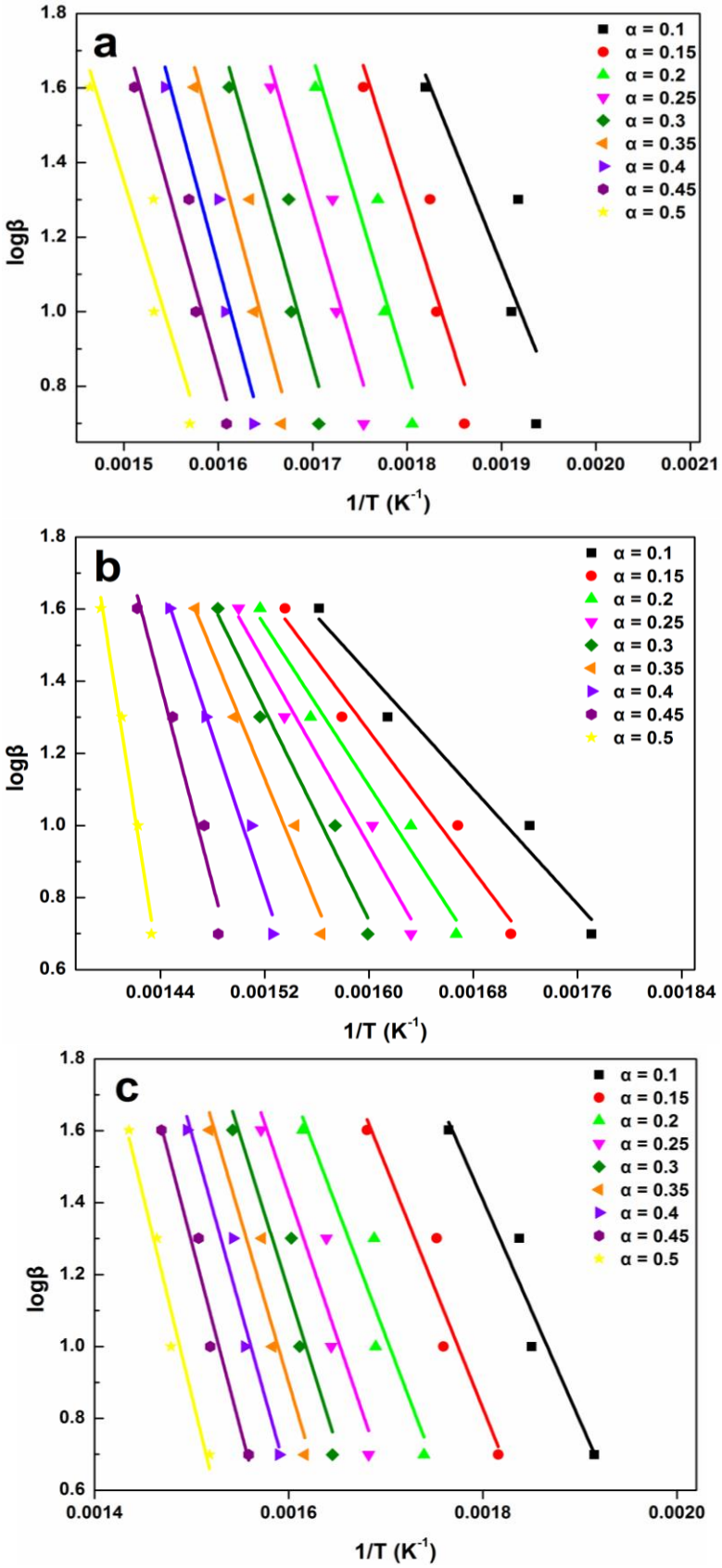

Fig. 4. Kinetic plots for determination of activated energy using FWO model at different conversions; (a) FLs, (b) WTs, (c) FLs/WTs

Table 4. Activation Energy Obtained from KAS and FWO Models for the Individual Sample and the Blends

α	FLs			
	KAS		FWO	
	E (kJ mol^{-1})	R^2	E (kJ mol^{-1})	R^2
0.1	112.14	0.54	115.08	0.59
0.15	143.80	0.79	145.52	0.81
0.2	151.99	0.80	153.58	0.82
0.25	156.39	0.77	158.02	0.80
0.3	162.72	0.77	164.30	0.80
0.35	170.41	0.80	171.83	0.82
0.4	170.41	0.84	172.02	0.86
0.45	163.96	0.85	166.08	0.86
0.5	146.71	0.79	149.96	0.80
Average	153.17	0.77	155.15	0.80
α	WTs			
	KAS		FWO	
	E (kJ mol^{-1})	R^2	E (kJ mol^{-1})	R^2
0.1	66.34	0.95	72.59	0.96
0.15	82.20	0.96	87.92	0.97
0.2	96.09	0.96	101.32	0.97
0.25	110.72	0.96	115.39	0.97
0.3	129.07	0.96	132.99	0.97
0.35	156.95	0.97	159.69	0.97
0.4	197.08	0.97	198.05	0.97
0.45	253.81	0.95	252.25	0.95
0.5	429.43	0.98	426.11	0.98
Average	169.08	0.96	171.81	0.97
α	FLs/WTs			
	KAS		FWO	
	E (kJ mol^{-1})	R^2	E (kJ mol^{-1})	R^2
0.1	108.58	0.90	111.86	0.92
0.15	119.46	0.87	122.66	0.88
0.2	126.45	0.81	129.70	0.84
0.25	142.58	0.82	145.33	0.84
0.3	155.58	0.85	157.90	0.87
0.35	165.39	0.89	167.38	0.90
0.4	174.78	0.93	176.47	0.93
0.45	186.62	0.94	187.91	0.95
0.5	201.15	0.95	201.98	0.95
Average	153.40	0.88	155.69	0.90

In the case of fallen leaves, the values obtained were 153.17 and 155.15 kJ mol^{-1}, for using the KAS and FWO models, respectively, which was close to the sawdust and pinewood and superior to moso bamboo in the previous literature (Chen *et al.* 2014a; Mishra *et al.* 2015; Wang and Zhao 2016). For the co-pyrolysis of FLs/WTs, it appeared that the average values in the two models were much closer to the FLs itself and far from the WTs, which possibly involved a synergistic effect between fallen leaves and waste tires. In other words, biomass may act as a hydrogen donor during co-pyrolysis, which can explain the formation of free radicals from biomass pyrolysis and participate in reactions of polymer decomposition (Abnisa and Wan 2014; Zhou *et al.* 2009). In general, the reason why the activation energy of FLs alone was lower than the solely WTs was due to their

difference in the contents of elemental components and macromolecular structures (Ma *et al.* 2015).

After consideration of the activation energy, another kinetic parameter was estimated by using the Coats-Redfern model (Ceylan and Topçu 2014). The results of the pre-exponential factor are shown in Table 5 with four different heating rates. The solid fuels pyrolysis was assumed as a first-order reaction and substituted average activation energy values into a fitted intercept as ln($AR/\beta E$) (Chin *et al.* 2014).

Table 5. Calculated Pre-exponential Factors (A, s^{-1})

Sample	5 °C/min		10 °C/min		20 °C/min		40 °C/min	
	KAS	FWO	KAS	FWO	KAS	FWO	KAS	FWO
FLs	1.02E7	1.03E7	1.27E7	1.29E7	1.19E7	1.20E7	2.31E7	2.34E7
WTs	2.05E7	2.09E7	5.68E7	5.77E7	3.92E9	3.98E9	3.78E10	3.84E10
FLs/WTs	8.37E6	8.49E6	1.27E7	1.29E7	1.08E7	1.09E7	2.32E7	2.35E7

CONCLUSIONS

1. Pyrolysis is a complex reaction process. According to the TG/DTG profiles, it was observed that in the presence of structural difference, the thermal degradation of FLs was recognized as three stages, while the WTs pyrolysis mechanism resulted in a single major stage.
2. The mixing of fallen leaves and waste tires in the course of co-pyrolysis had a noticeable effect on both the thermal decomposition reactions and kinetic behaviors when compared with the pyrolysis of each individual feedstock. This suggested that there was a synergistic effect through radical interactions between biomass fallen leaves and waste tires.
3. The quantitative determination of activation energies and pre-exponential factors of three samples revealed a reaction process and mechanism. Simultaneously, combined with the results of ultimate analysis, it can be concluded that fallen leaves mixed with waste tires could be used as energy feedstock.

ACKNOWLEDGMENTS

The authors are grateful for the Natural Science Foundation of Jiangsu Province (Grant No. BK20161524), the Doctorate Fellowship Foundation of Nanjing Forestry University (2015), the Jiangsu Province Ordinary University Students' Scientific Research Innovation Project (KYZZ16_0319), the National Natural Science Foundation of China (Grant No. 31400515), and the Priority Academic Program Development of Jiangsu Higher Education Institutions (PAPD). Also, this paper was sponsored by the Qing Lan Project.

REFERENCES CITED

Abnisa, F., and Wan, A. (2015). "Optimization of fuel recovery through the stepwise co-pyrolysis of palm shell and scrap tire," *Energy Conversion & Management* 99, 334-345. DOI: 10.1016/j.enconman.2015.04.030

Abnisa, F., and Wan, M. (2014). "A review on co-pyrolysis of biomass: An optional technique to obtain a high-grade pyrolysis oil," *Energy Conversion & Management* 87, 71-85. DOI: 10.1016/j.enconman.2014.07.007

Brebu, M., Ucar, S., Vasile, C., and Yanik, J. (2010). "Co-pyrolysis of pine cone with synthetic polymers," *Fuel* 89(8), 1911-1918. DOI: 10.1016/j.fuel.2010.01.029

Bridgwater, A. V. (2004). "Biomass fast pyrolysis," *Thermal Science* 8(2), 21-49. DOI: 10.2298/TSCI0402021B

Bridgwater, A. V. (2012). "Review of fast pyrolysis of biomass and product upgrading," *Biomass & Bioenergy* 38(2), 68-94. DOI: 10.1016/j.biombioe.2011.01.048

Cai, J. Q., Wang Y. P., Zhou L. M., Huang Q. W. (2008). "Thermogravimetric analysis and kinetics of coal/plastic blends during co-pyrolysis in nitrogen atmosphere," *Fuel Processing Technology* 89(1), 21-27. DOI: 10.1016/j.fuproc.2007.06.006

Cao, L., Yuan, X., and Jiang, L. (2016). "Thermogravimetric characteristics and kinetics analysis of oil cake and torrefied biomass blends," *Fuel* 175, 129-136. DOI: 10.1016/j.fuel.2016.01.089

Çepelioğullar, Ö., and Pütün, A. E. (2013). "Thermal and kinetic behaviors of biomass and plastic wastes in co-pyrolysis," *Energy Conversion & Management* 75(11), 263-270. DOI: 10.1016/j.enconman.2013.06.036

Çepelioğullar, Ö., Haykırıaçma, H., and Yaman, S. (2015). "Kinetic modelling of RDF pyrolysis: Model-fitting and model-free approaches," *Waste Management* 48, 275-284. DOI: 10.1016/j.wasman.2015.11.027

Ceylan, S., and Topçu, Y. (2014). "Pyrolysis kinetics of hazelnut husk using thermogravimetric analysis," *Bioresource Technology* 156(4), 182-188. DOI: 10.1016/j.biortech.2014.01.040

Chen, D. Y., Zhou, J. B., and Zhang, Q. S. (2014a). "Effects of heating rate on slow pyrolysis behavior, kinetic parameters and products properties of moso bamboo," *Bioresource Technology* 169(5), 313-319. DOI: 10.1016/j.biortech.2014.07.009

Chen, D. Y., Zhou, J. B., and Zhang, Q. S. (2014b). "Torrefaction of rice husk using TG-FTIR and its effect on the fuel characteristics, carbon, and energy yields," *BioResources* 9(4), 135-143. DOI: 10.15376/biores.9.4.6241-6253

Chen, D., Zhou, J, B., and Zhang, Q. S. (2014c). "Upgrading of rice husk by torrefaction and its influence on the fuel properties," *BioResources* 9(4), 5893-5905.

Chen, W. M., Shi, S. K., Nguyen, T., and Zhou, X. Y. (2016a). "Effect of temperature on the evolution of physical structure and chemical properties of bio-char derived from co-pyrolysis of lignin with high-density polyethylene," *BioResources* 11(2), 3923-3936. DOI: 10.15376/biores.11.2.3923-3936

Chen, W. M., Shi, S. K., Zhang, J., and Zhou, X. Y. (2016b). "Co-pyrolysis of waste newspaper with high-density polyethylene: Synergistic effect and oil characterization," *Energy Conversion & Management* 112, 41-48. DOI: 10.1016/j.enconman.2016.01.005

Chin, B. L. F., Yusup, S., and Shoaibi, A. A. (2014). "Kinetic studies of co-pyrolysis of rubber seed shell with high density polyethylene," *Energy Conversion & Management* 87, 746-753. DOI: 10.1016/j.enconman.2014.07.043

Doyle, C. D. (2003). "Estimating isothermal life from thermogravimetric data," *Journal of Applied Polymer Science* 6(24), 639-642. DOI: 10.1002/app.1962.070062406

El-Sayed, S. A., and Mostafa, M. E. (2014). "Pyrolysis characteristics and kinetic parameters determination of biomass fuel powders by differential thermal gravimetric analysis (TGA/DTG)," *Energy Conversion & Management* 85(85), 165-172. DOI: 10.1016/j.enconman.2014.05.068

El-Sayed, S. A., and Mostafa, M. E. (2015). "Kinetic parameters determination of biomass pyrolysis fuels using TGA and DTA techniques," *Waste and Biomass Valorization* 6(3), 401-415. DOI: 10.1007/s12649-015-9354-7

Gustafsson, C., and Richards, T. (2009). "Pyrolysis kinetics of washed precipitated lignin," *BioResources* 4(1), 26-37.

Huang, X., Cao, J. P., and Zhao, X. Y. (2015). "Pyrolysis kinetics of soybean straw using thermogravimetric analysis," *Fuel* 169(4), 93-98. DOI: 10.1016/j.fuel.2015.12.011

Ma, Z. Q., Chen, D. Y., and Gu, J. (2015). "Determination of pyrolysis characteristics and kinetics of palm kernel shell using TGA-FTIR and model-free integral methods," *Energy Conversion & Management* 89, 251-259. DOI: 10.1016/j.enconman.2014.09.074

Martínez, J. D., Puy, N., and Murillo, R. (2013). "Waste tyre pyrolysis – A review," *Renewable & Sustainable Energy Reviews* 23, 179-213. DOI: 10.1016/j.rser.2013.02.038

Martínez, J. D., Veses, A., and Mastral, A. M. (2014). "Co-pyrolysis of biomass with waste tyres: Upgrading of liquid bio-fuel," *Fuel Processing Technology* 119(1), 263-271. DOI: 10.1016/j.fuproc.2013.11.015

Mishra, G., Kumar, J., and Bhaskar, T. (2015). "Kinetic studies on the pyrolysis of pinewood," *Bioresource Technology* 182, 282-288. DOI: 10.1016/j.biortech.2015.01.087

Montiano, M. G., Díaz-Faes, E., and Barriocanal, C. (2016). "Kinetics of co-pyrolysis of sawdust, coal and tar," *Bioresource Technology* 205, 222-229. DOI: 10.1016/j.biortech.2016.01.033

Mui, E. L., Cheung, W. H., and Lee, V. K. (2010). "Compensation effect during the pyrolysis of tyres and bamboo," *Waste Management* 30(5), 821-830. DOI: 10.1016/j.wasman.2010.01.014

Oasmaa, A. (1999). "Fuel oil quality of biomass pyrolysis oils-state of the art for the end users," *Energy & Fuels* 13(4), 914-921. DOI: 10.1016/S0140-6701(00)96592-5

Quek, A., and Balasubramanian, R. (2013). "Liquefaction of waste tires by pyrolysis for oil and chemicals – A review," *Journal of Analytical & Applied Pyrolysis* 101(5), 1-16. DOI: 10.1016/j.jaap.2013.02.016

Rivilli, P. L., Yranzo, G. I., and Pérez, J. D. (2011). "Stepwise isothermal fast pyrolysis (SIFP) of biomass. Part I. SIFP of pine sawdust," *BioResources* 6(3), 2703-2710. DOI: 10.1007/s10973-014-4179-3

Shafiee, S., and Topal, E. (2009). "When will fossil fuel reserves be diminished?," *Energy Policy* 37(1), 181-189. DOI: 10.1016/j.enpol.2008.08.016

Uçar, S., and Karagöz, S. (2014). "Co-pyrolysis of pine nut shells with scrap tires," *Fuel* 137, 85-93. DOI: 10.1016/j.fuel.2014.07.082

Uzun, B., and Yaman, E. (2014). "Thermogravimetric characteristics and kinetics of scrap tyre and Juglans regia shell co-pyrolysis," *Waste Management & Research* 32(10), 961-970. DOI: 10.1177/0734242X14539722

Wang, J., and Zhao, H. (2016). "Error evaluation on pyrolysis kinetics of sawdust using iso-conversional methods," *Journal of Thermal Analysis and Calorimetry* 124(3), 1635-1640. DOI: 10.1007/s10973-016-5308-y

White, J. E., Catallo, W. J., and Legendre, B. L. (2011). "Biomass pyrolysis kinetics: A comparative critical review with relevant agricultural residue case studies," *Journal of Analytical and Applied Pyrolysis* 91(1), 1-33. DOI: 10.1016/j.jaap.2011.01.004

Williams, P. T. (2013). "Pyrolysis of waste tyres: A review," *Waste Management* 33(8), 1714-1728. DOI: 10.1016/j.wasman.2013.05.003

Zhou, L., Luo, T., and Huang, Q. (2009). "Co-pyrolysis characteristics and kinetics of coal and plastic blends," *Energy Conversion & Management* 50(3), 705-710. DOI: 10.1016/j.enconman.2008.10.007

Zhu, F., Feng, Q., and Xu, Y. (2015). "Kinetics of pyrolysis of ramie fabric wastes from thermogravimetric data," *Journal of Thermal Analysis & Calorimetry* 119(1), 651-657. DOI: 10.1007/s10973-014-4179-3

Article submitted: January 5, 2017; Peer review completed: March 26, 2017; Revised version received and accepted: May 1, 2017; Published: May 15, 2017.
DOI: 10.15376/biores.12.3.4707-4721